The effects of hexabromocyclododecane on the transcriptome and hepatic enzyme activity in three human HepaRG-based models

Susana Proença [a,b,*,1], Nick van Sabben [a], Juliette Legler [a], Jorke H. Kamstra [a,2], Nynke I. Kramer [a,b,2]

[a] *Department of Toxicology, Institute for Risk Assessment Sciences, Utrecht University, Utrecht, the Netherlands*
[b] *Toxicology Division, Wageningen University, Wageningen, the Netherlands*

ARTICLE INFO

ABSTRACT

The disruption of thyroid hormone homeostasis by hexabromocyclododecane (HBCD) in rodents is hypothesized to be due to HBCD increasing the hepatic clearance of thyroxine (T4). The extent to which these effects are relevant to humans is unclear. To evaluate HBCD effects on humans, the activation of key hepatic nuclear receptors and the consequent disruption of thyroid hormone homeostasis were studied in different human hepatic cell models. The hepatoma cell line, HepaRG, cultured as two-dimensional (2D), sandwich (SW) and spheroid (3D) cultures, and primary human hepatocytes (PHH) cultured as sandwich were exposed to 1 and 10 μM HBCD and characterized for their transcriptome changes. Pathway enrichment analysis showed that 3D models, followed by SW, had a stronger transcriptome response to HBCD, which is explained by the higher expression of hepatic nuclear receptors but also greater accumulation of HBCD measured inside cells in these models. The Pregnane X receptor pathway is one of the pathways most upregulated across the three hepatic models, followed by the constitutive androstane receptor and general hepatic nuclear receptors pathways. Lipid metabolism pathways had a downregulation tendency in all exposures and in both PHH and the three cultivation modes of HepaRG. The activity of enzymes related to PXR/CAR induction and T4 metabolism were evaluated in the three different types of HepaRG cultures exposed to HBCD for 48 h. Reference inducers, rifampicin and PCB-153 did affect 2D and SW HepaRG cultures' enzymatic activity but not 3D. HBCD did not induce the activity of any of the studied enzymes in any of the cell models and culture methods. This study illustrates that for nuclear receptor-mediated T4 disruption, transcriptome changes might not be indicative of an actual adverse effect. Clarification of the reasons for the lack of translation is essential to evaluate new chemicals' potential to be thyroid hormone disruptors by altering thyroid hormone metabolism.

1. Introduction

Hexabromocyclododecane (HBCD) is a mixture of very lipophilic and (thermo)stable diastereomers and was the third most used brominated flame retardant by 2001, accounting for 8.2 % of total market demand (Alaee et al., 2003; Morose, 2006; Nixon, 1997). However, its potential to bioaccumulate and biomagnify and its possible endocrine disruptive properties, led to the inclusion of HBCD in the list of Substances of Very-High Concern of the Stockholm Convention (ECHA, 2008). Although this classification has led to a decrease in worldwide HBCD production, emissions of HBCD will continue due to HBCD's persistency in the environment and the long shelf-lives of products containing HBCD

(Li and Wania, 2018).

Concerns about HBCD being an endocrine disruptor, specifically of thyroid hormones, came after chronic and subchronic toxicity studies in rats showed increased liver weights, changed thyroid morphology, reduced thyroxin (T4), and increased thyroid stimulating hormone (TSH) levels (Ema et al., 2008; van der Ven et al., 2006). Additionally, HCBD induced the expression and activity of biotransformation enzymes CYP2B, CYP3A and UGT, affected membrane transporters' expression and decreased the expression of genes involved in cholesterol biosynthesis and lipid metabolism in the liver (Cantón et al., 2008; Farmahin et al., 2019; Germer et al., 2006; Shockley et al., 2020; van der Ven et al., 2006). The profile of hepatic enzymes induced by HBCD points to the activation of hepatic nuclear factors pregnane X receptor (PXR) and constitutive androstane receptor (CAR) (Daujat-Chavanieu and Gerbal-Chaloin, 2020).

Fig. 1 summarizes the hypothesized mechanism in literature by which HBCD disrupts thyroid hormone homeostasis in the liver (Hennemann et al., 2001; Jansen et al., 2005; Noyes et al., 2019; van der Spek et al., 2017). PXR/CAR activation induces the expression of membrane transporters including MCT8 and OATP1B1, and the activity of phase 2 enzymes, UGTs and SULTs. Higher levels of these transporters and elevated enzymatic activity may enhance T4 clearance. Less T4 is subsequently converted into the biologically active triiodothyronine (T3), leading to increases in thyroid stimulating hormone (TSH) levels, the overactivation of the thyroid and disruption of thyroid hormone signaling pathways. Other PXR/ CAR inducers such as rifampicin, carbamazepine and phenytoin, have been associated to thyroid hormone disruption in human patients in clinical cases, corroborating the relevance of this mechanism of thyroid hormone disruption for humans (Christensen et al., 1989; Curran and Leslie, 1991; Ohnaus et al., 1981; Zhang et al., 2016).

However, there is some uncertainty about the translation of HBCD-induced effect on T4 levels from rats to humans (Foster et al., 2021; Noyes et al., 2019; Plummer et al., 2021). A 48 h exposure to 25 μM HBCD led to increased levels of PXR-regulated *CYP3A4* mRNA expression in both rat (H4IIE) and human (HepG2) hepatoma cell lines and primary rat hepatocytes (Fery et al., 2009). However, in the human model, HBCD (up to 15 μM) did not induce CYP3A4 activity, while it did in rat hepatocytes (Fery et al., 2009). Additionally, no transcriptome changes were observed in an alveolar epithelial cell line (A549) and C3A subclone of HepG2 exposure to respectively 2 and 4 μM HBCD for 48 h (Zhang et al., 2015).

Whether HBCD does affect T4 hepatic clearance in human hepatocytes specifically has not been tested yet. In fact, in vitro studies of human hepatic metabolism of thyroid hormones are scarce. Richardson

et al. (2014) studied deiodination, glucuronidation and sulfate conjugation using rat and primary human hepatocytes (PHH). These authors showed that PCB-153, a known thyroid hormone disruptor in rats (Liu et al., 2012), induced T4 glucuronidation in PHH. More recently, 3D models of HepaRG cells were tested on their capacity to synthesize thyroid binding serum proteins and metabolize T4 through glucuronide or sulfate conjugation (Kühnlenz et al., 2022). This study illustrated the potential of using human in vitro hepatocyte models for screening chemicals disruption of T4 metabolism.

Given the ambiguous effects of HBCD exposure in HepG2 and the lack of data regarding HBCD effects on T4 hepatic metabolism in human cell systems, the present study aims to assess HBCD effects on human hepatic gene expression and activity of enzymes related to PXR induction and T4 clearance using more hepatic-like human in vitro models. The expected outcomes of this study were the clarification of whether HBCD effects are hepatic cell model dependent and if HBCD is a T4 disruptor in humans through hepatic mechanisms. HepaRG cells, a human hepatoma cell line known for its robust hepatic phenotype, and primary human hepatocytes (PHH) from mixed donors were used to study these effects (Gerets et al., 2012; Guillouzo et al., 2007). In addition to the standard 2D monolayers, HepaRG cells were cultured as sandwich (SW) cultures and spheroids (3D), which enhances the cell-cell and cell-ECM interactions, resulting in a more hepatocyte-like phenotype compared to 2D cultures (Gunness et al., 2013a; Mueller et al., 2014; Wang et al., 2014). The concentrations of 1 and 10 μM HBCD were used based on the previous in vitro studies (Germer et al., 2006; Hamers et al., 2006; Wang et al., 2016; Zhang et al., 2015). To assess the effects of HBCD on these hepatocyte models and culture techniques, we first evaluated the transcriptomic response and secondly, we measured enzyme activity levels for CYP3A4, UGTs and T4 glucuronidation, sulfation and deiodination. For validation of the induction of CYP3A4 activity we used rifampicin and for induction of T4 glucuronidation we used PCB-153, as this chemical has been shown to increase T4 glucuronidation in human hepatocytes (Richardson et al., 2014). Finally, the concentration of the three HBCD isomers, α, β and γ HBCD, was measured in cells over time to help explain differences in sensitivity to HBCD between the three HepaRG models. HBCD isomers are differentially cleared (Wang et al., 2021) and lipophilic and therefore cell concentrations over time are likely to differ between isomer and cell system (Kramer et al., 2015; Proença et al., 2021).

2. Materials and methods

2.1. Chemicals and reagents

An HBCD technical mixture (CAS 134237–5–6) was obtained as a composite mix through Bromine Science and Environmental Forum (BSEF) (van der Ven et al., 2006). Dimethyl sulfoxide (DMSO, D8418), insulin (I6634), α-HBCD (30373), rifampicin (R3501), 7-hydroxycoumarin (U7626), 7-hydroxycoumarin glucuronide (UC263), T4 (T-2501) and collagenase type I (SCR103) were obtained from Sigma-Aldrich. T3 (T-074), reverse T3 (T-075) and 1-hydroxymidazolam (H-922) were obtained as certified reference materials from Cerilliant while T4 glucuronide (T425630) was obtained from Toronto Research Chemicals and T4 sulfate conjugate (HY-101406) from Med Chem Express. Midazolam was purchased from Spuyt Hillen. Fetal Bovine serum (10270–106), 0.05% trypsin-EDTA (25300054), penicillin and streptomycin (15140–122), glutamine (25030–024), Insulin-Transferrin-Selenium (ITS, 41400045) and Hank's balanced salt solution buffer (HBSS, 14025092) were obtained from Gibco. Williams' E medium without phenol red and L-Glutamine (A1217–01) was obtained from ThermoFisher and hydrocortisone 21-hemisuccinate (SC-250130) from Santa Cruz. The 48-well microplates were obtained from Greiner. The 96-well round bottom (7007), the 24-well flat bottom (CLS3473–24EA) ultra-low attachment (ULA) plates, the Matrigel (356231) and rat tail collagen type I (354249) were obtained from
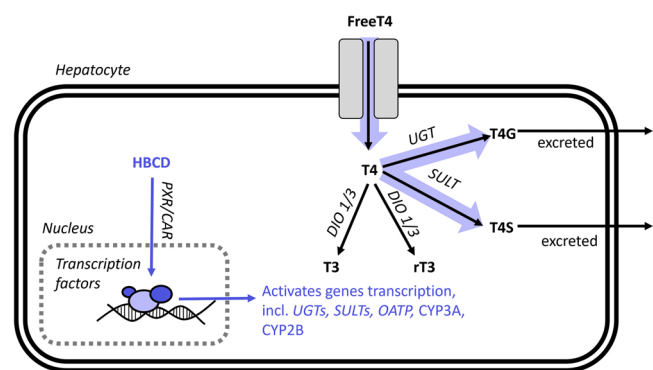
Fig. 1. Scheme of the current proposed mechanism through which HBCD affects T4 clearance: 1) HBCD enters the cell and activates PXR and /or CAR nuclear receptors. The nuclear receptor(s) migrate to the cell nucleus where together with other transcription factors it activates the transcription of several genes including UGTs, SULTs, etc. The induction of expression of Phase II enzymes and T4 membrane transporters accelerates the overall clearance of T4.

Corning® Costar®. HepaRG (HPR101) were obtained from Biopredic and PHH (X008001-P, LiverPooled Cryoplateable Hepatocytes) from BioIVT. Analytical standards, α-HBCD, 7-hydroxycoumarin, 7-hydroxycoumarin glucuronide, T4, T3, reverse T3, T4 glucuronide and sulfate, midazolam and 1-hydroxymidazolam were all equal or above 97% purity.

2.2. HepaRG maintenance and 2D culture

Undifferentiated HepaRG cells (Biopredic) were routinely cultured up to passage 22 in Phenol Red-free Williams' E medium supplemented with 10 % fetal bovine serum, 100 IU/mL penicillin, 100 μg/mL streptomycin, 872 nM insulin, 2 mM glutamine, and 50 μM hydrocortisone 21-hemisuccinate (Gerets et al., 2012; Pomponio et al., 2015). After reaching confluency, cells were differentiated for ten days in culture medium supplemented with 1% DMSO. Then, cells were trypsinized and 65,000 cells per well were seeded for 2D cultures in 48 well plates.

2.3. HepaRG SW culture

In SW cultures, first plates were coated with 50 μL of 1.5 mg/mL rat tail collagen type I. Afterwards, 130,000 cells/well were seeded on top of the collagen and then overlayed with 50 μL 1.5 mg/mL Matrigel in 48 well plates (Dong and Smith, 2009; Gross-Steinmeyer et al., 2005).

2.4. HepaRG 3D cultures

To create spheroids, 1800 cells were seeded in each well of a 96-well round bottom ultra-low attachment (ULA) plate and centrifuged for 4 min at 200 xG (Bell et al., 2016; Ramaiahgari et al., 2017).

2.5. Differentiation and exposure of HepaRG cultures to HBCD

The three culture were incubated in DMSO-free culture medium at 37 °C and 5% CO_2 and 48 h after the medium was replaced with culture medium containing 2% FBS and 1 % DMSO (Pomponio et al., 2015). After 96 h seeding, medium was replaced again and 120 h after seeding cells were exposed to chemicals. The relatively high percentage of DMSO in the exposure medium is deemed acceptable since DMSO 1–2 % is used for hepatocytes differentiation (Gerets et al., 2012). Four-days after seeding 24 spheroids were pooled and added into each well of a 24-well ULA microplate. Exposure to chemicals was initiated 120 h after seeding. The exposure scenarios for each assay are summarized in Fig. 2.

2.6. Primary human sandwich hepatocytes

Four batches of mixed-gender primary human hepatocytes pooled from 10 donors were thawed and 175,000 viable cells were plated in each well of a 48-well plate in between layers of collagen type I and Matrigel, using the same protocol as for HepaRG SW cultures. Cultures were exposed to test chemicals 72 h after seeding.

2.7. Transcriptomics analysis

HepaRG cultures and PHH were exposed to 1 or 10 μM HBCD or vehicle (1 % DMSO) for 24 h or repeatedly every 48 h. After exposure, cells were lysed using 1X TempO-Seq Lysis Buffer, and frozen lysates were shipped to Bioclavis (Glasgow, Scotland) where the TempO-Seq assay was conducted using the EU-ToxRisk v2.1 panel (3565 probes) (Limonciel et al., 2018). For 2D and SW HepaRG cultures and PHH, two wells of the same condition were pooled together while for 3D cultures only one well was used. Four independent replicates were made for each condition.

Unsupervised clustering techniques, principal component analysis (PCA) (factoextra package[3]) and a hierarchical clustering (pheatmap package[4]) were performed using variance stabilizing transformed read counts from all cellular models (cell models comparisons) and separate cell models (exposure specific comparisons). These analyses identified possible outlier samples. Analyses of differentially expressed genes and functional analysis were made on separate files per cellular model and exposure length (24 or 48 h). Normalization of the read counts and differential expression were performed using the Deseq2 method (Love et al., 2014) and a design formula that included the biological replicate and type of exposure (chemical, concentration and length of exposure).

Differential expression (DE) was measured by the Wald-s test, shrunken following the apeglm method (Zhu et al., 2019), and p-values adjusted by the Benjamini-Hochberg (FDR) method. Each DE analysis was evaluated by creating histograms of the p-values, and log2 fold change (Supplemental Fig. S2). Gene set enrichment analysis (GSEA) analyses were performed using Webgestalt (Wang et al., 2017) and using Wikipathways as a database for reference pathways. For GSEA, ranking of genes was performed based on the sign of log2 fold change and -log10 (p-value). For gene specific analysis, we used DE genes with p-adjusted values of < 0.05. For enriched pathways, we considered a false discovery rate value < 0.05 as significant.

2.8. CYP3A4 and UGT activity

The three HepaRG cultures were exposed for 24 h to vehicle (1 % DMSO, minimum level of DMSO required for differentiation), 1 μM HBCD, 10 μM HBCD, 10 μM rifampicin (prototypical PXR inducer) or 5 μM PCB-153 (prototypical inducer of T4 glucuronidation). After exposure to HBCD or prototypical inducers for 24 h, cells were exposed again to the same concentration of HBCD or prototypical inducers together with the CYP3A4 substrate, midazolam (5 μM), the UGT substrate 7-hydroxycoumarin (3 μM), or 1 μM T4. To assess whether supplementation of selenium would increase deiodinase activity of T4, some experiments were performed with medium supplemented with 5 % ITS instead of the insulin supplementation, from day 2 of culture and throughout HBCD, PCB-153 and T4 exposure.

At the start of exposure of substrates or T4 and at each timepoint, exposure medium samples were collected and diluted in the same volume of methanol in 1.5 mL short-thread auto-sampler glass vials and kept in the − 20 °C prior to chemical analysis. The three HepaRG cell models were exposed to midazolam for 2, 4 and 8 h and 7-hydroxycoumarin for 1, 2 and 4 h. 2D and SW cultures were exposed for 24 h to T4. The 3D models were exposed to T4 for 48 h because metabolites were not detected after 24 h exposure. Cells, in addition to medium, were collected from HepaRG exposed to T4. For this, 2D HepaRG cultures were incubated with 100 μL/well 0.05 % trypsin/EDTA at 37 °C for 10 min. Cell suspensions in trypsin/EDTA were transferred to glass 1.5 mL autosampler vials with 100 μL cold acetonitrile. For SW cultures, 2 mg/mL of collagenase type I in HBSS was added to cells and incubated at 37 °C for 10 min. Then cells with collagenase were collected in autosampler vials with glass inserts and centrifuged for 10 min and 500xG. The supernatant was carefully removed and 100 μL acetonitrile was added to cells. For 3D cultures, cells were collected with the remaining medium to glass vial inserts. Samples were centrifuged for 5 min at 500 xG, the supernatant removed and 100 μL cold acetonitrile was added to cells. All samples were vortexed and stored at − 20 °C.

2.9. In vitro distribution of HBCD

To evaluate the metabolism and distribution of HBCD in different in vitro compartments, medium, cells and plastic samples were collected

---

[3] https://cran.r-project.org/web/packages/factoextra/index.html
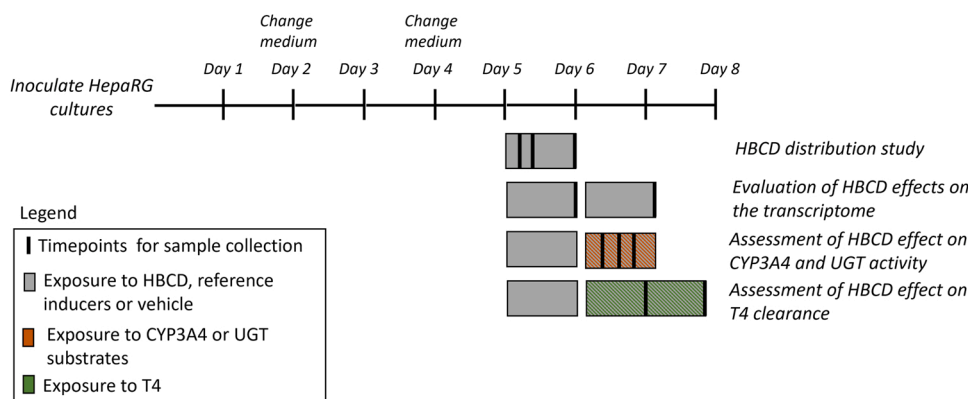[4] https://cran.r-project.org/web/packages/pheatmap/pheatmap.pdf

Fig. 2. Schematic representation of the exposure scenarios used for the different assays in this paper. The three different HepaRG cultures were exposed on day 5 and 6 to HBCD, vehicle or positive controls. For the study of HBCD mass balance and cell exposure, samples were collected after 4, 8 and 24 h acute exposure. For the transcriptomics, after 24 single exposure and 24 h after the second exposure. For the CYP3A4 substrates experiment, medium samples were collected 2, 4 and 8 h. For the UGT substrate experiment, medium samples were collected after 1, 2 and 4 h. For T4 metabolism and cellular accumulation, samples of medium and cells were collected after 24 h in 2D and SW HepaRG cultures and 48 h in 3D HepaRG cultures.

after 4, 8 and 24 h of exposure to 10 μM HBCD. Medium and cell samples were collected as referred to in the previous section. To collect the HBCD associated with plastic, 0.25 mL and 0.5 mL of methanol were added to each well of the 48-well and 24 -ULA well plates, respectively. Plates were covered with parafilm and incubated for two hours at room temperature and with 250 rpm orbital agitation. Thereafter, methanol was transferred to glass vials and stored at – 20 °C.

2.10. Analytical measurements

Standards for LC-MS/MS analysis of α-HBCD, midazolam 1-hydroxymidazolam, 7-hydroxycoumarin, 7-hydroxycoumarin glucuronide, T4, T3, reverse T3 (rT3), T4 glucuronide (T4G) and T4 sulfate conjugate were prepared in the same matrix as the cell, plastic and medium extracts. Isomers of HBCD were separated by retention time and assumed to have the same concentration-signal response as α-HBCD. Before analysis, extracts were centrifuged for 10 min at 12,000 xG to precipitate and/or separate any protein. A Shimadzu triple-quadrupole system with two Nexera XR LC-20 CE pumps, a Nexera XR SIL-20AC autosampler, a CTO-20AC column oven, an FCV-20AH2 valve unit, and LCMS-8050, a GraceSmart RP18 5 μM 150 mm × 2.1 mm (GreatSmart) column and Luna 3 μM C18(2) 100 mm × 3.0 mm (Luna) column were used to measure chemical concentrations. Peaks were integrated using the LabSolution Insight™ software. The LC-MS/MS methods are further described in Supplemental Table S1.

Technical triplicates for 2D and SW and technical duplicates for 3D were assessed. Three independent biological replicates for the three cell models were used. To compare clearance and intracellular accumulation of HBCD between the cell models, HBCD amounts were normalized to cell number, and counted using trypan blue staining. Plots and statistical analysis were performed using GraphPad Prism version 9.0.0 for Windows, GraphPad Software, San Diego, California USA.

3. Results

3.1. Global transcriptomic profiles show differences between models, but not between controls and HBCD treatment

Using transcriptomics analyses, we assessed the differences in gene expression levels between unexposed cell models and between HBCD-exposed and unexposed cell models. PCA of all the samples indicated that most of the variation in expression levels is contained in PC1 (Fig. 3a). PC1 separated PHH samples from HepaRG models. The separation of the 2D, SW and 3D HepaRG cultures was more visible along the PC2 axis. SW and 3D models clustered closer together than the 2D cultures. Samples of PHH spread across PC2, indicating a larger variation in expression levels between PHH samples than between HepaRG samples.

To confirm that HepaRG 3D and SW cultures had a more hepatic phenotype than the 2D cultures, we compared expression levels of key

hepatic genes in unexposed HepaRG and PHH (Fig. 3b). The *PXR* and *CAR* expression levels of 3D HepaRG model were not statistically different from PHH levels. SW and 2D HepaRG cultures had an identical expression of these nuclear receptors which was less than 0.5 fold of the PHH expression levels. Peroxisome proliferator-activated receptor (*PPAR-α*) gene expression levels were not statistically different in PHH, 3D and SW HepaRG models after 24 h exposure to vehicle (Ann Barretto et al., 2019; Pavek, 2016; Pavek, 2016). Hepatic Nuclear factor 4-α (*HNF4-α*) expression was significantly lower in all HepaRG culture models compared to PHH. The 3D and SW HepaRG cultures had similar expression levels, 0.5–0.25 fold lower than PHH, and 2D HepaRG culture had *HNF4-α* expression 0.125 fold lower than PHH. There was no discernible difference in aryl hydrocarbon receptor (*AhR*) gene expression levels. (Legendre et al., 2009; Vorrink and Domann, 2014) *HIF1-α* was the only gene that was more highly expressed in 2D cultures than in the other cell models, 2.8 fold higher than PHH. In general, the hepatic gene expression profile of the 3D HepaRG model most resembled that of PHH, followed by SW.

The PCA and hierarchical clustering heatmap analysis of the separate models did not show clustering of samples based on HBCD and vehicle exposure, indicating that HBCD exposure did not cause extensive changes in the transcriptome profile (Fig. 3c, d, e and f and Supplemental-Fig. S1). For some models, the PCA showed the existence of clusters based on other factors, such as biological replicate and exposure duration to HBCD or vehicle The variation in gene expression in PHH was related to the length of exposure while HepaRG seems to have more biological replicates inter-variation, especially for the 2D HepaRGcultures (Supplemental-Fig. S1). This analysis together with additional quality control checks (e.g. p-value histograms, Supplemental Fig. S2) informed the design for DESeq2 analysis described in the methods section.

3.2. HBCD induces hepatic nuclear receptor mediated toxicity pathways

In agreement with the unsupervised clustering analysis, DE analysis indicates that HBCD exposure had limited effects on overall gene expression (Supplemental Fig. S2 and S3). The PHH cell models appears to be especially unaffected by HBCD after 48 h exposures. Furthermore, none of the cell models had a clear relationship between the fold change of DE genes and concentration or length of exposure to HBCD. Hence, instead of focusing on individual DE genes (also presented in Supplemental Fig. S4 and S5), we investigated global gene changes related to biological pathways through GSEA. Fig. 4a illustrates the significantly (p-value<0.05) changed pathways per cell model for at least one of the exposure scenarios. There was no overlap of any significantly enriched pathways across all cell models. The nuclear receptors reported to be induced by HBCD, PXR and CAR, were significantly enriched in all HepaRG cultures and in SW and 3D HepaRG cultures, respectively.

To explore this further, Fig. 4b gives the enrichment score of these
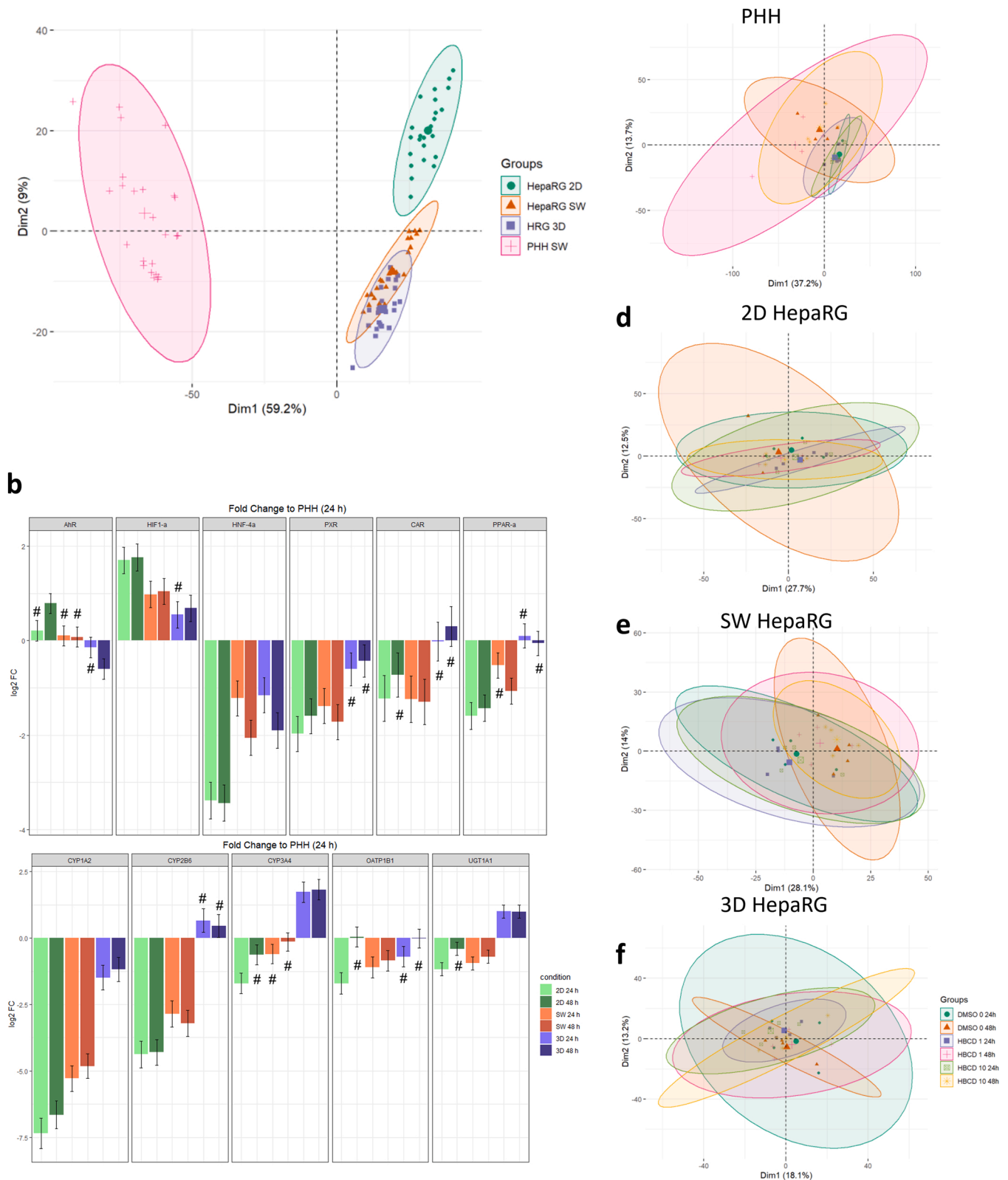
Fig. 3. Overview of transcriptomics differences between the three HepaRG models and PHH model and between vehicle and 1 and 10 μM HBCD exposure for 24 and 48 h. a - Results of PCA analysis of the four cell models, exposed to vehicle or HBCD, shown as the distribution of samples across PC1 and 2. Ellipse formation and coloring were based on the culture cell models. b – Log2 fold change of key hepatic genes in HepaRG model relative to PHH exposed to vehicle (1% DMSO) for 24 h. The symbol # identifies fold changes that had a p-adjusted value > 0.05. Results of individual PCA analysis of the c - PHH, d - 2D HepaRG, e - SW HepaRG, and **f** - 3D HepaRG exposed to vehicle or HBCD, shown as the distribution of samples across PC 1 and 2. Ellipse formation and color were based on the exposure condition.

a

3D HepaRG

PHH

- Novel intracellular components of RIG-I-like receptor (RLR) pathway
- Eicosanoid metabolism via Cytochrome P450 Mono-Oxygenases (CYP) pathway Type II interferon signaling (IFNG)

- Ethanol effects on histone modifications
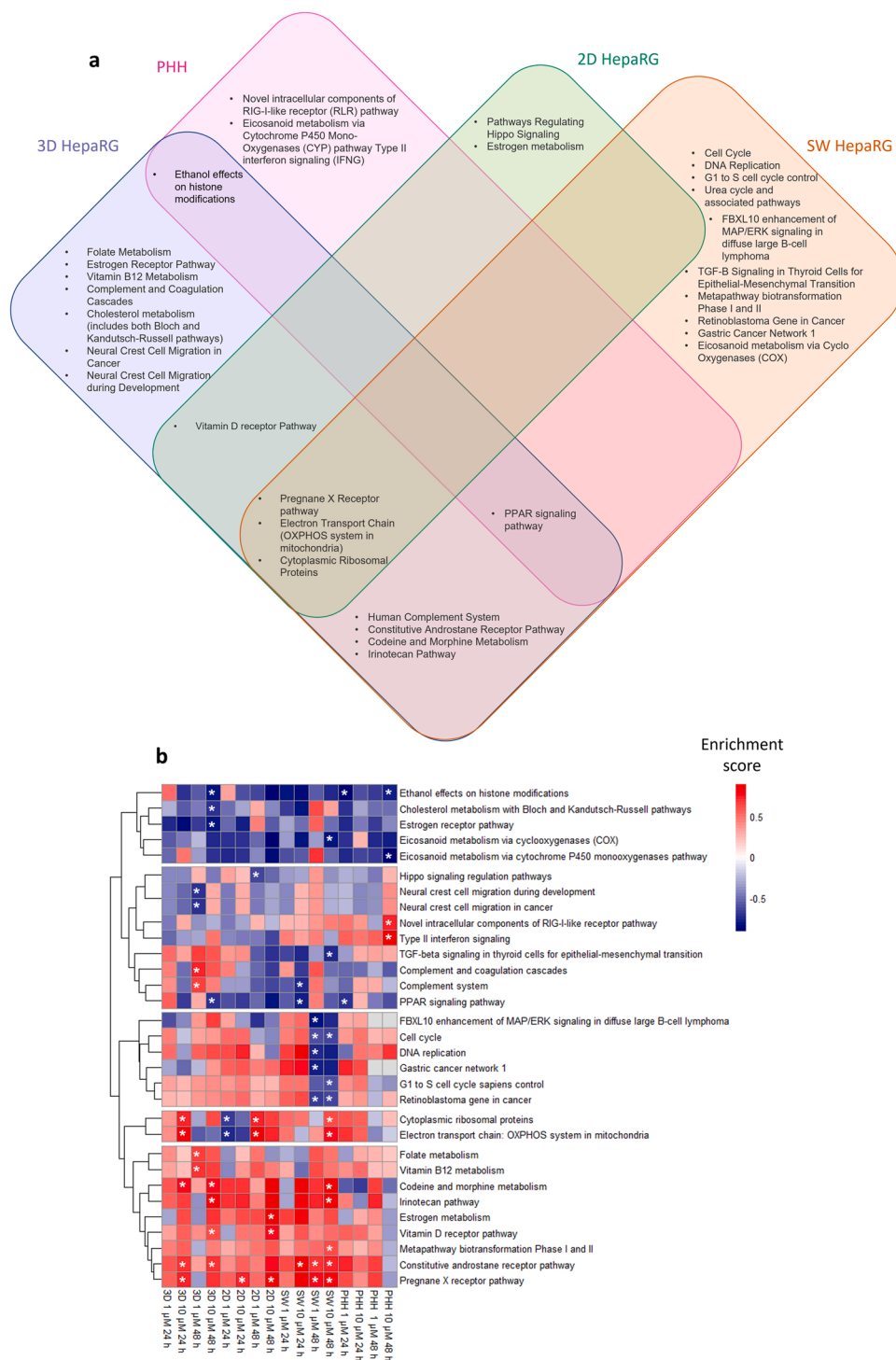
- Folate Metabolism
- Estrogen Receptor Pathway
- Vitamin B12 Metabolism
- Complement and Coagulation Cascades
- Cholesterol metabolism (includes both Bloch and Kandutsch-Russell pathways)
- Neural Crest Cell Migration in Cancer
- Neural Crest Cell Migration during Development

2D HepaRG

- Pathways Regulating Hippo Signaling
- Estrogen metabolism

SW HepaRG

- Cell Cycle
- DNA Replication
- G1 to S cell cycle control
- Urea cycle and associated pathways
- FBXL10 enhancement of MAP/ERK signaling in diffuse large B-cell lymphoma
- TGF-B Signaling in Thyroid Cells for Epithelial-Mesenchymal Transition
- Metapathway biotransformation Phase I and II
- Retinoblastoma Gene in Cancer
- Gastric Cancer Network 1
- Eicosanoid metabolism via Cyclo Oxygenases (COX)

- Vitamin D receptor Pathway

- Pregnane X Receptor pathway
- Electron Transport Chain (OXPHOS system in mitochondria)
- Cytoplasmic Ribosomal Proteins

- PPAR signaling pathway

- Human Complement System
- Constitutive Androstane Receptor Pathway
- Codeine and Morphine Metabolism
- Irinotecan Pathway

b

Enrichment score

Fig. 4. Wikipathways resulting from GSEA of PHH and HepaRG 2D, SW and 3D models exposed to HBCD in several conditions: 1 and 10 μM for single dose for 24 h and 1 and 10 μM for double dose in a total of 48 h. a - Venn diagram of the pathways significantly enriched (FDR<0.05) in each cell model for at least one exposure conditions. b - Heatmap and dendrogram illustrating the pathways hierarchical clustering (created by pheatmap R function) for all the pathways significantly enriched at least in one condition in once cell model. Colors in heatmap go from red for high positive enrichment score to blue for low negative enrichment score. White asterisk symbolize significance (FDR<0.05).

pathway analyses across all cell models, timepoints and HBCD concentration (a positive score indicates an upregulated pathway and a negative score indicates a downregulated pathway). In 3D and 2D HepaRG models, the PXR pathway has a higher enrichment score after exposure to 10 μM HBCD than after 1 μM HBCD, suggesting a concentration-dependent response. The SW models show stronger enrichment at both concentrations after 48 h than for 24 h. The PXR pathway is not significantly enriched in the PHH model. PXR activation induces the transcription of genes of key biotransformation enzymes including *CYP2B6*, *3A4/5/7* and *UGT1A1* (Supplemental Fig. S4). The 3D and SW models also show the induction of *ABCA1* and *ABCB1*, important

transporter genes in lipid homeostasis, and *HSP90AA1*, which encodes for a chaperone that complexes with PXR or CAR for activating their responsive elements in the DNA. Furthermore, the PXR gene itself is induced after HCBD exposure in the SW model. Despite not being significantly induced in all three HepaRG models, CAR, the metapathway biotransformation Phase I and II, Vitamin D receptor (VDR) and Estrogen metabolism pathways cluster with the PXR pathway, and are consistently induced upon HBCD exposure. In fact, some of these pathways consist of mostly the same genes present in the PXR pathway (e.g., *CYP3A4, CYP2B6* and *ABCB1*) (Supplemental Table S2). The metapathway biotransformation Phase I and II includes hepatic enzymes

such as *AKR1B10* and *1C3*, *CYP4F3*, *GRX2*, *SULT1B1* and *1C2*, *UGT1A10* and *UGT2B15*. The VDR pathway also includes *SPP1* (secreted phosphoprotein 1), *S100A9* (S100 Calcium Binding Protein A9), *MYC* and *SULT1C2*, among other genes.

Similarly to ethanol effects on histone modifications, more pathways were predominantly downregulated after HBCD exposure, including cholesterol and eicosanoid metabolism (Fig. 4b). Unlike the mostly upregulated pathways, the downregulated pathways have much less overlap of genes (Supplemental File 2). Related to these pathways, the genes *CYP2E1* and *CYP4A11* were the most consistently downregulated genes. Overall, the profile of these downregulated pathways cluster points towards HBCD affecting lipid homeostasis and estrogen regulation (Supplemental Figs. S4 and Supplemental Table S2). Additionally, while all HepaRG models had a significantly enriched cytoplasmic ribosomal protein pathway and electron transport chain (OXPHOS system in mitochondria) after HBCD exposure, the enrichment direction was not consistent (Fig. 4b).

3.3. Effect of HBCD on CYP3A4 and UGT enzyme activity in different HepaRG models

To assess whether gene expression changes translated into activity changes, we proceeded to characterize the influence of HBCD and reference inducers rifampicin and PCB-153 on the activity of CYP3A4, UGTs and other enzymes involved in T4 metabolism.

In 2D HepaRG culture, CYP3A4 and UGT activity followed first-order kinetics, as demonstrated by midazolam depletion and 1-hydroxymidazolam formation for CYP3A4, and 7-hydroxycoumarin depletion and glucuronide formation for UGTs (Fig. 5a and d). As expected, rifampicin induced CYP3A4 in the 2D HepaRG culture. HBCD exposure, however, did not induce CYP3A4 or 7-hydroxycoumarin glucuronidation. In fact, 10 µM HBCD seemed to slightly decrease the rate of midazolam depletion and its 1-hydroxymidazolam formation.

There was more CYP3A4 and UGT activity in SW cultures, than in 2D cultures (Fig. 5b and e). Unlike in the 2D HepaRG culture, levels of 1-
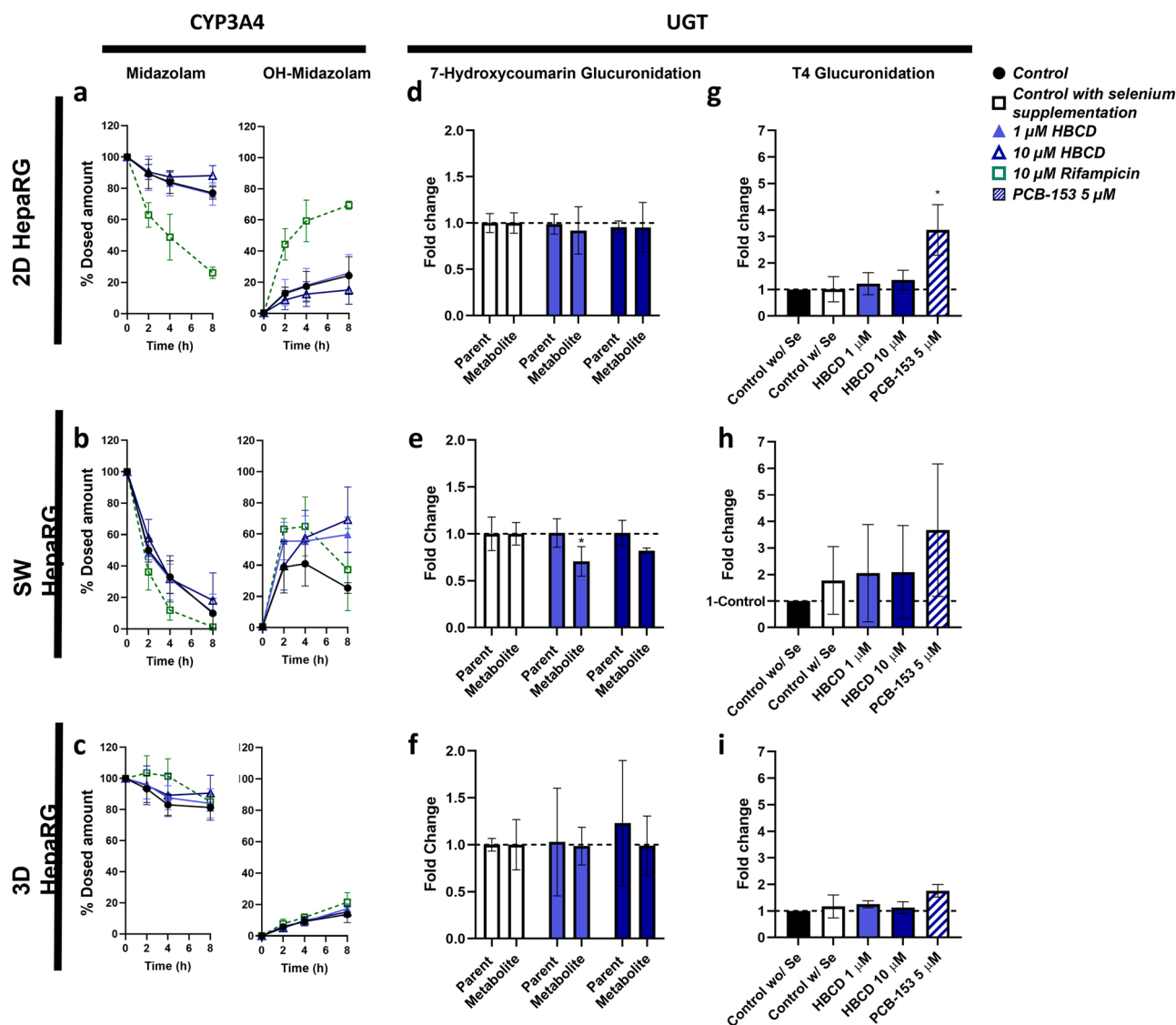

Fig. 5. - Enzymatic activity of 2D, SW and 3D cultures of HepaRG cells after exposure to vehicle control, HBCD and reference inducers, Rifampicin for CYP3A4 induction and PCB-153 for T4 glucuronidation induction. a, b and c - CYP3A4 enzymatic activity as measured by depletion of midazolam and formation of its main metabolite, 1-hydroxymidazolam (1-OH midazolam); d, e and f - Fold change of 7-hydroxycoumarin (7-OH coumarin) glucuronidation throughout four hours as measured by the parent compound depletion and metabolite formation in medium. Glucuronidation was calculated as first order kinetics in 2D and SW cultures and as a zero-order kinetic in 3D cultures g, h and i- Fold induction of T4 glucuronidation based on T4G formation after 24 exposure to the different chemicals relative to control without Se supplementation (no statistical difference of vehicle control with selenium). Dots and bars represent the average of 3 independent replicates and standard deviation. Statistical significance was calculated by ANOVA relative to e control and g control with Selenium supplementation.

hydroxymidazolam in the medium of SW cultures did not steadily increase over time, even decreasing after 4 h exposure to the vehicle control. Although rifampicin increased midazolam depletion and 1-hydroxymidazolam formation relative to control, the amount of 1-hydroxymidazolam decreased after 4 h exposure (Fig. 5b). HBCD did not affect midazolam depletion in SW cultures, but it affected 1-hydroxymidazolam formation; there was more metabolite in HBCD exposed wells for all timepoints than in control. Notably, the observed kinetics of 1-hydroxymidazolam result in a recovery of midazolam and metabolite lower than 100 % after 8 h of incubation (ranging from a minimum of 35–87 % for SW cells exposed to vehicle control and 10 μM HBCD, respectively). HBCD did not affect 7-hydroxycoumarin depletion in SW cultures, but it did cause a slight decrease in the formation of its metabolite (statistically significant for 1 μM).

In the 3D model of HepaRG, HBCD exposure did not affect the clearance of midazolam or 7-hydroxycoumarin (Fig. 5C and F). Rifampicin exposure also did not induce CYP3A4 activity. Substrate depletion

and metabolite formation (not normalized by cell number) were slower in the 3D system than in the 2D and SW cultures and followed close to zero-order kinetics, indicating possible saturation of the observed metabolic pathways. This could explain the absence of change in activity after HBCD and rifampicin exposure.

To study the effect of HBCD on T4 metabolism, we followed the extent to which T4 depletion from medium, T4 cellular uptake, and formation of several metabolites were affected by HBCD exposure. Despite the role of selenium in deiodination, supplementation of ITS did not affect T3 and rT3 formation. In general, exposure to HBCD or PCB-153 did not lead to altered T4 uptake or even total T4 (sum of T4 medium and cells) depletion in any of the three HepaRG cultures (Supplemental Fig. S5). The apparent decrease of T4 recovery in 3D cultures exposed to 10 μM HBCD or PCB-153 was not statistically significant. In general, T4 cellular uptake was higher in SW and 3D cultures, respectively 10 % and 14.5 % of the dosed amount compared to 4.9 % in the 2D cultures. This cellular uptake in SW and 3D cell models caused a slight
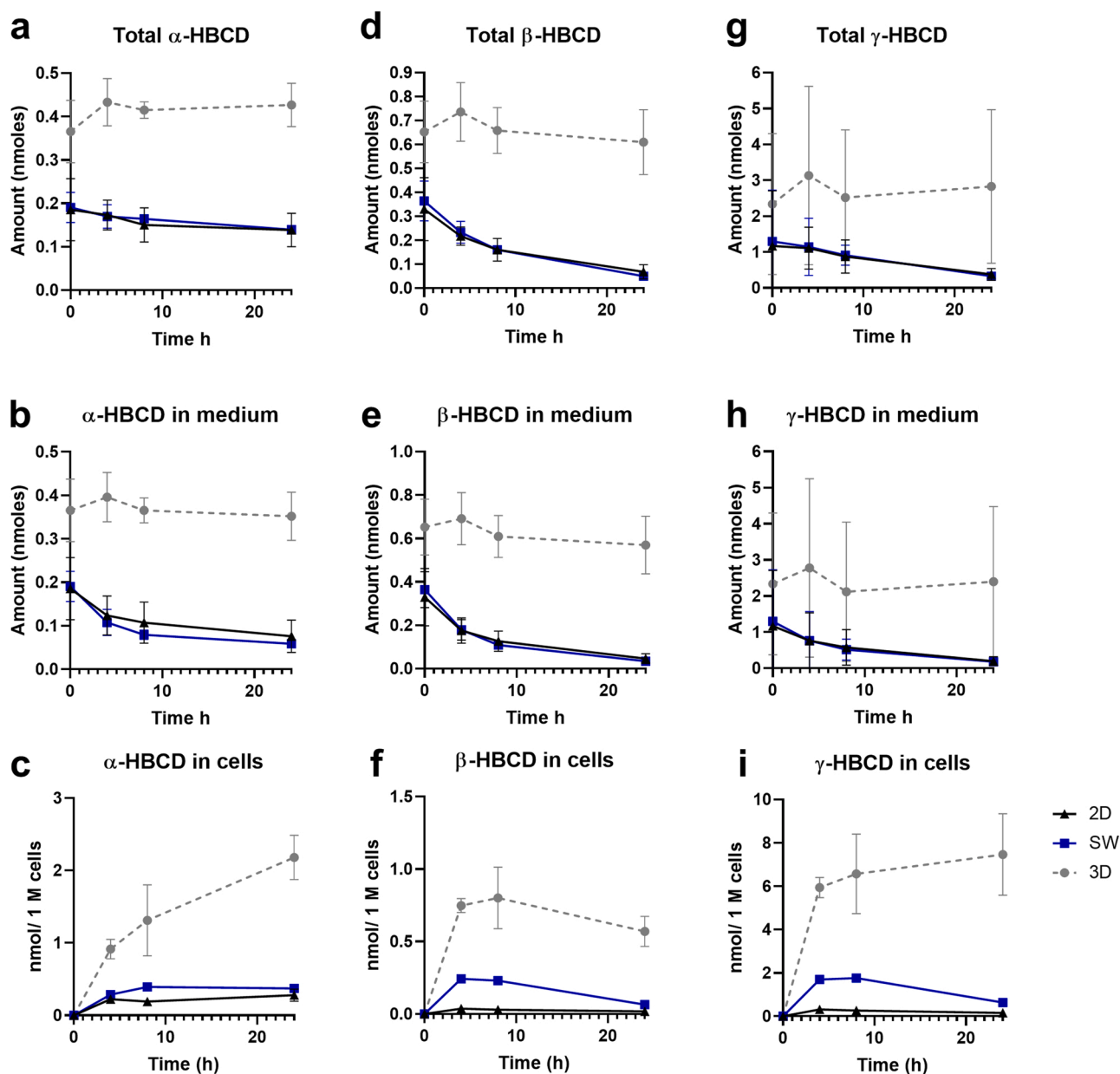

Fig. 6. Profile and quantity of HBCD three isomers, α-HBCD, β-HBCD and γ-HBCD, throughout 24 h as a - total amount (sum of medium, plastic and cells), b - as amount in medium and c - as concentration in cells. Plots show as dots the average independent replicates with the standard deviation and lines show the average tendency.

depletion of T4 from the medium after 24 and 48 h, respectively. No rT3 or T4-Sulfate conjugate was detected in any of the cell models and exposure conditions. There was T3 present in medium samples even before exposure to cells, as a contaminant (around 0.24 %) of the parent compound, T4. The residual increase of T3 after exposure to cells was too close to basal levels (never higher than 0.37 % of dosed T4) to make an accurate evaluation of differences in T3 formation.

T4 glucuronide was the only quantifiable metabolite in the three HepaRG models (Fig. 5g, h and i). In the 2D cultures 0.19 % of T4 was converted to T4G after 24 h. In SW cultures this percentage was 1.29 and in 3D cultures, after 48 h, T4G amounted to 0.74 % of T4 initial dose. No effect of either dose of HBCD in the T4G formation in 2D, SW and 3D HepaRG cultures was found, whereas the positive control PCB-153 significantly increased T4G formation by 3.2-fold in 2D cells. There was also higher T4G in SW and 3D cultures exposed to PCB-153, but these levels were not significantly different from controls (p > 0.05, ANOVA).

3.4. Nominal and cell-associated HBCD concentrations not proportional

To ascertain whether a difference in intracellular HBCD levels between cell models helps explain differences in HBCD effects between these models, concentrations of each isomer associated with the cells after 24 h of exposure to 10 μM of HBCD were analytically determined.

According to the supplier, the HBCD mixture used in this study is composed of 10.28 % α-HBCD, 8.72 % β-HBCD, and 81.01 % γ-HBCD. Analytically determined levels of α-HBCD and β-HBCD in exposure medium were reproducible across replicates. However, levels of γ-HBCD in medium after 0 and 24 h exposure varied greatly across biological replicates for all three cultures (6.4–112 %). In contrast, the amount of γ-HBCD in cells and plastic after 24 h exposure was consistent across replicates (Fig. 6 and Supplemental Fig. S6).

The recovery of α-HBCD and β-HBCD in the wells without cells (amount of HBCD in medium and plastic) for the three HepaRG models was between 80% and 120%; (Supplemental Fig. S6). However, recovery of the total amount of α-HBCD and β-HBCD from 2D and SW cultures (sum of the amount in medium, plastic and cells) was much lower (Fig. 6a,d and g). For β-HBCD isomer in 2D and SW cultures, the rate of depletion of the total amount and the amount in the medium was similar. This indicates that β-HBCD depletion in the medium was mostly due to metabolism. Oppositely, the amount of α-HBCD in the medium decreased more extensively than the total amount of α-HBCD. In this case α-HBCD depletion is due to two processes, metabolism and distribution to cells. Plastic was not a significant sink (<5 % of the dosed amount) for any of the three HBCD isomers, especially in the presence of cells. The amount of total HBCD in cells also never reached more than 5 % of the initial dosed amount. The profile of β and γ-HBCD in cells throughout time, as illustrated in Fig. 6c, f and i, was similar between the 2D, SW, and 3D cultures; the isomers quickly accumulated in cells within 4 h, after which they slightly decreased or reached a steady-state. The profile of α-HBCD accumulation in cells is different between the culture models; while for 2D and SW cultures, there is a steady state after 4 h of exposure, for 3D cells, there is a continuous increase of α-HBCD. Normalizing the amount of the HBCD isomers in cells per cell number shows that the 3D system had the highest intracellular exposure to the three HBCD isomers (Supplemental Table S4). Cells in SW culture had slightly higher exposure to HBCD than 2D cells.

4. Discussion

The influence of HBCD on the induction of PXR/CAR pathways and hepatic biotransformation pathways associated with T4 clearance has been explored in rodent models. Studies of the effects of HBCD on human hepatocyte models are few and results are ambiguous. PXR may be activated by HBCD in human hepatocytes, but changes in gene expression and activity of key biotransformation enzymes have not been

reported (Fery et al., 2009; Zhang et al., 2015; Fery et al., 2009; Zhang et al., 2015). Previous studies used the HepG2 cell line, with poor biotransformation enzyme induction capabilities (Gerets et al., 2012; Westerink and Schoonen, 2007). Therefore, the first objective of this study was to assess what hepatic model would be more suitable for screening the potential of chemicals perturbing T4 metabolism.

In this study, we evaluated the suitability of HepaRG cell line cultured as standard 2D, sandwich (SW) and spheroid (3D) cultures. This evaluation first consisted in the comparison of transcriptome of control and HBCD-exposed HepaRG cultures and PHH SW cultures. Then we assessed the activity and induction of biotransformation enzymes of the HepaRG cultures. The hepatic genes chosen for this characterization, consisted of Phase 1 and 2 enzymes but also key nuclear receptors. PXR, CAR, AhR and PPAR-α were included due to being common targets of hepatic toxicants. Hepatic Nuclear factor 4-α (HNF4-α) was chosen because it acts as a co-factor of PXR and CAR-mediated transcriptional activation (Pavek, 2016). Hypoxia-induced factor 1 -α (HIF 1-α) is not a specific hepatic nuclear receptor but is an important inhibitor of some of the other pathways (e.g. AhR and CAR) (Legendre et al., 2009; Vorrink and Domann, 2014). Based on our transcriptomics analysis, the 3D model had the most hepatic phenotype. In line with published literature (Gunness et al., 2013b; Lauschke et al., 2016), gene expression patterns in our 3D cultures most resembled those in PHH, especially PXR and CAR-pathway associated genes. Next, we tested for the thyroid hepatic metabolism and the activity of CYP3A4 and UGTs, enzymes regulated by PXR and CAR using prototypical substrates in the three HepaRG models. In accordance with our gene expression profiles, the enzymatic activity, normalized to cell number[5], was significantly higher in 3D cultures compared to 2D and SW cultures (Supplemental Table S3). However, in contrast to 2D and SW cultures, no induction of CYP3A4 and T4 glucuronidation by prototypical inducers rifampicin and PCB-153 was observed. The 3D model had low cell numbers relative to exposure medium volume, which resulted in easy enzyme saturation at the tested substrate concentrations and therefore hampered the detection of activity induction.

To our knowledge, there are only few studies of T4 clearance in human hepatocytes specifically (Kühnlenz et al., 2022) in PHH and in a co-culture of HepaRG (Richardson et al., 2014). Taking into account the different number of cells, the T4 depletion, intracellular uptake and glucuronidation, are similar between the PHH used in Richardson et al. (2014) and the HepaRG culture used here, especially in SW and 3D cultures. The co-culture model of Kühnlenz et al. (2022) also did detect a quantity of T4 comparable to the SW and 3D HepaRG cultures used in this study. However, in our HepaRG cultures there was no detection of T4S, possibly due to the relative high limit of quantification. Kühnlenz et al. (2022) did not report the formation of T3 and rT3 in their HepaRG co-cultures and with the HepaRG used here, rT3 was not detected and T3 formation was considered insignificant. The addition of selenium to the medium, which is essential for the synthesis of selenoproteins such as deiodinases (Schomburg, 2012), did not affect the deiodination of T4. On the other hand, PCR data (not shown here) revealed that HepaRG expresses deiodinase-1 (*DIO-1*) and *OATP1B1* mRNA and so, these cells should be capable of representing all the T4 metabolic pathways observed in vivo. In summary the setup for the 3D cultures improved the phenotype but, in this case, reduced the sensitivity to detect inducers in metabolite depletion experiments. This capacity to detect enzymes activity induction is essential for identifying T4 metabolism disruptors and so, in our study 2D and SW appear to be more suitable models. Still, for future studies screening for chemicals disrupting T4 metabolism, medium composition, including selenium formulations and

---

[5] For better clarity herein we emphasize the difference between the intrinsic metabolic activity, which is related to the expression of the enzymes, and the metabolic capacity of the cell models, which depends on the intrinsic metabolic activity and the ratio number of cells/volume of medium.

thyroxin-binding globulin, should be first optimized.

Finally, using the three different HepaRG models, we sought to clarify the effects of HBCD in human hepatocytes. However, since the three HepaRG models' set-up and metabolic capacity differs, the evaluation of HBCD intracellular exposure in the different cell models is an important step to understand the differences sensitivities to HBCD effects. In general, the profiles of HBCD isomers metabolism in this study are similar to what was previously observed in the literature, the isomers are differently metabolized and are highly bioaccumulative (Erratico et al., 2016; Wang et al., 2021). For γ-HBCD, the variation in medium hampered the evaluation of the clearance rate and cellular uptake. Since the samples of γ-HBCD in cells and plastic for the same experimental wells did not had such problematic variation and neither did the samples for the two other HBCD isomers, the issue appears to be analytical. The cause for the issue in the analytical detection of γ-HBCD was not identified but could be related to the fact that each diastereomer of HBCDS is also a mixture of stereoisomers (Erratico et al., 2016). The 3D model appears to have much higher intracellular exposure than SW and 2D, possibly due to their relative low cell numbers (fewer cells to collect HBCD from medium (Gülden et al., 2001)), but also the low ratio of the number of cells and volume of medium, which results in a lower metabolic capacity of the model. Although the exposure of PHH to HBCD was not measured, it is expected it had the lowest exposure due to the higher numbers of cells and higher cells' intrinsic metabolic activity (based on PHH hepatic enzymes gene expression and *in house* data for enzymatic activity for specific substrates). It should be noted that we evaluated the uptake and clearance only for the first 24 h of exposure, while a second exposure (as performed with transcriptomics and enzymatic activity assays) causes more cellular accumulation of HBCD on top of the already accumulated amount.

First the effect of HBCD on the hepatic cell models was evaluated through transcriptomics, more specifically, by performing a GSEA. Of the three HepaRG models, SW and 3D cultures appear to have the most pathways significantly enriched after HBCD exposure. The low number of pathways significantly enriched by HBCD in 2D HepaRG model was possibly due to lower expression of relevant hepatic nuclear receptors and enzymes, and/or lower intracellular exposure to HBCD. The small of effect of HBCD on PHH transcriptome might indicate the different cell types have different sensitivity to HBCD. However, the holistic analysis of changed pathways in all models, concentrations, and timepoints, as shown in Fig. 4b, shows very consistent similarities, especially for the cluster of induction of PXR and CAR pathway but also the cluster of inhibition of ethanol effects on histone modifications. Possible reasons for the absence of the effect of HBCD on PHH transcriptome are the lowest intracellular exposure of all models or the higher variability present in PHH (as observed in PCA). These results highlight the importance of assessing the actual exposure of cells to the toxicant and of having a high number of biological replicates in transcriptomics analysis.

The PXR and CAR pathways are some of the most consistently and strongly induced pathway by HBCD in HepaRG cells, which corroborates with earlier studies. The correlation of these two pathways and also Vitamin D receptor pathway (VDR) is due to a large overlap of the genes constituting the pathways. PXR, CAR and VDR constitute group I of subfamily 1. These nuclear receptors have very similar DNA-binding domains and co-activation of their pathways has been reported (Pavek, 2016). Whether the interaction of HBCD with other human nuclear receptors is direct or indirect can be clarified with reporter gene assays, which has been done for a few nuclear receptors (Hamers et al., 2006), albeit not for human CAR.

HBCD also downregulated pathways related to lipid metabolism in the HepaRG models. Especially *CYP2E1* and *CYP4A11*, enzymes involved in these pathways, are strongly inhibited. This effect on lipid metabolism is also corroborated by literature since subacute exposure to HBCD caused inhibition of PPAR-regulated genes involved in lipid metabolism in mixed gender rats. In female rats, there was also

inhibition of genes involved in estrogen metabolism (Cantón et al., 2008). While Canton et al. (2008) discussed that PPAR pathway inhibition could be due to the decrease of T4, this mechanism is unlikely to occur with the in vitro models used herein. Alternatively, it has been proposed that the PXR/CAR activation inhibits PPAR-α activation through competition of coactivator peroxisome proliferator–activated receptor g coactivator 1α (Shizu et al., 2021). Since PPAR-α is involved in lipid metabolism, the inhibition of the pathway possibly explains the inhibition of cholesterol metabolism and ethanol effects on histone modifications pathways (Varga et al., 2011). Still, the exact sequence of events through which HBCD causes lipid metabolism dysregulation in hepatocytes is not clear. Studies with HepG2 cells exposed to HBCD did show an accumulation of phospholipids and eicosanoid acids possibly via inhibition of long-chain fatty acid β-oxidation (Wang et al., 2016). CYP2E1 is not regulated by PPAR-α but its inhibition could be related to the decrease of acetone found in the same study. Acetone is a known inducer of CYP2E1 and a by-product of fatty acids metabolism (Koop and Casazza, 1985). This data all together point to HBCD being a possible inducer of metabolic dysfunction associated with fatty liver disease in humans. This would also explain some of the immune and stress related pathways (e.g. NRF-2, type II interferon signaling, and complement system induced by HBCD in this and other studies (Gannon et al., 2019)).

Given that PXR was the most consistently changed pathway, along with induction of the CYP3A family, CYP2B6 and UGT1A1, we assessed the functionality of this pathway by using different functional assays. These assays showed that the effects of HBCD on the transcriptome did not translate into enzymatic activity. Induction of CYP3A4 expression by HBCD did not result in faster oxidation of midazolam in any of the models. This is in agreement with results obtained with HepG2 exposed to HBCD (Fery et al., 2009). Similarly, induction of some UGTS expression did not cause faster glucuronidation of either 7-hydroxycoumarin or T4. Here, we propose three possible explanations for the lack of translation of gene expression to activity. Firstly, there are several processes between mRNA expression and protein synthesis, and translocation into the endoplasmic reticulum membrane (Feder and Walser, 2005). One or several of these processes might not proceed proportionally to the increased expression of the specific gene. Another explanation is based on UGTs being functionally redundant (Soars et al., 2004). T4, 7-hydroxycoumarin and 1-hydroxymidazolam are substrates of several UGTs (den Braver-Sewradj et al., 2017; Hyland et al., 2009; Tong et al., 2007). The slight increase of some of these UGTs might not reflect on actual higher total glucuronidation, since other mechanisms (e.g., intracellular uptake of chemical) might be the limiting step. There are reports of T4 clearance being limited by the rate of cellular transport, although this is not consensual (Hennemann et al., 2001; Jansen et al., 2005). A third possible explanation is that HBCD simultaneously binds to UGTs and/or CYP3A4, inhibiting the activities of these enzymes and annulling the induction of enzyme activity resulting from a higher expression of the enzymes (Wei et al., 2016). The abnormal kinetic profile of 1-hydroxymidazolam in the SW cultures provides some evidence for this hypothesis. Midazolam is metabolized by CYP3A4 into 1-hydroxymidazolam that is eventually glucuronidated (Nguyen et al., 2016). The absence of a continuous increase of 1-hydroxymidazolam in the SW cultures exposed to vehicle and rifampicin can be due to glucuronidation, which depleted the phase I metabolite. Following this rationale, the continuous increase of 1-hydroxymidazolam in the HBCD-exposed cells indicates there is less glucuronidation. The slight inhibition of 7-hydroxycoumarin glucuronidation (observed only in metabolite formation) in SW cultures exposed to both concentrations of HBCD (Fig. 5d) further supports this hypothesis. In fact, HBCD isomers are metabolized mostly CYP3A4 (Erratico et al., 2016) and in this study, there are indications of (10 μM) HBCD inhibiting CYP3A4 activity in the 2D cultures (Erratico et al., 2016). Thus, constituting evidence of potential for competitive inhibition. It is noteworthy that rifampicin, here tested and PXR and CYP3A4 positive inducer, has shown to not induce

T4 glucuronidation in co-cultures of HepaRG cells (Kühnlenz et al., 2022).

In conclusion, despite the evidence that HBCD causes thyroid hormone disruption in rodents by inducing its hepatic metabolism, this effect does not translate to in vitro models with human hepatocytes. These results highlight the uncertainties related to translating thyroid hormone disruptive activities from rodent studies to humans. Unraveling the profiles of human PXR and CAR inducers in inducing different UGTs and consequently T4 clearance, is a key step to identify potential human thyroid hormone disruptors. We highlight that, of our knowledge, only PCB-153 has been shown to affect T4 glucuronidation in vitro human hepatic models. Hence this chemical should be used to study the relevance of this mechanism of T4 disruption in humans.

The 3D HepaRG cultures had the most hepatic-like phenotype and thus, it is more promising for studies of inducibility of nuclear receptors and consequent enzymes upregulation. However, to perform an adequate assay of enzyme-activity induction, the number of cells per volume of medium is a factor as important as the hepatic phenotype of the cells. Therefore, it is a factor that needs equal consideration for future studies of these endpoints.

Notably, although HBCD may affect additional pathways related to thyroid hormones kinetics (e.g., displacement of T4 from serum proteins (Hamers et al., 2006)), epidemiological studies of HBCD exposure have led to inconclusive results on its effects on thyroid hormones, neurodevelopment and reproductive endpoints (EFSA panel on CONTAM, 2021). Given that in our study we found lipid metabolism to be affected by HBCD across the cell models (Fig. 4), future studies of HBCD effects in humans should focus on this hallmark and determine if HBCD represents a risk for liver toxicity in humans.

CRediT authorship contribution statement

SP, NK and JK conceived the study. SP and NvS collected the data, SP and NvS performed the analysis of the enzyme assays and SP and JK performed the analysis of the transcriptomics. JL, JK and NK supervised the findings of this work. All authors discussed the results and contributed to the final manuscript.

Declaration of Competing Interest

The authors declare that they have no known competing financial interests or personal relationships that could have appeared to influence the work reported in this paper.

Data availability

Data will be made available on request.

Appendix A. Supporting information

Supplementary data associated with this article can be found in the online version at doi:10.1016/j.tox.2022.153411.

References

Alaee, M., Arias, P., Sjödin, A., Bergman, Å., 2003. An overview of commercially used brominated flame retardants, their applications, their use patterns in different countries/regions and possible modes of release. Environ. Int. 29, 683–689. https://doi.org/10.1016/S0160-4120(03)00121-1.

Ann Barretto, S., Lasserre, F., Fougerat, A., Smith, L., Fougeray, T., Lukowicz, C., Polizzi, A., Smati, S., Régnier, M., Naylies, C., Bétoulières, C., Lippi, Y., Guillou, H., Loiseau, N., Gamet-Payrastre, L., Mselli-Lakhal, L., Ellero-Simatos, S., 2019. Gene expression profiling reveals that PXR activation inhibits hepatic PPARα activity and decreases FGF21 secretion in male C57BL6/J mice. Int. J. Mol. Sci. 20 https://doi.org/10.3390/ijms20153767.

Bell, C.C., Hendriks, D.F.G., Moro, S.M.L., Ellis, E., Walsh, J., Renblom, A., Fredriksson Puigvert, L., Dankers, A.C.A., Jacobs, F., Snoeys, J., Sison-Young, R.L., Jenkins, R.E., Nordling, Å., Mkrtchian, S., Park, B.K., Kitteringham, N.R., Goldring, C.E.P., Lauschke, V.M., Ingelman-Sundberg, M., 2016. Characterization of primary human hepatocyte spheroids as a model system for drug-induced liver injury, liver function and disease. Sci. Rep. 6, 1–13. https://doi.org/10.1038/srep25187.

Cantón, R.F., Peijnenburg, A.A.C.M., Hoogenboom, R.L.A.P., Piersma, A.H., van der Ven, L.T.M., van den Berg, M., Heneweer, M., 2008. Subacute effects of hexabromocyclododecane (HBCD) on hepatic gene expression profiles in rats. Toxicol. Appl. Pharmacol. 231, 267–272. https://doi.org/10.1016/j.taap.2008.04.013.

Christensen, H.R., Simonsen, K., Hegedüs, L., Hansen, B.M., Døssing, M., Hansen, J.M, J.P.K., 1989. Influence of rifampicin on thyroid gland volume, thyroid hormones, and antipyrine metabolism. Acta Endocrinol. 121.

Curran, P.G., Leslie, J., 1991. Thyroid hormones and the thyroid gland *. Endocr. Rev. 12, 135–150.

Daujat-Chavanieu, M., Gerbal-Chaloin, S., 2020. Regulation of CAR and PXR expression in health and disease. Cells https://doi.org/10.3390/cells9112395.

den Braver-Sewradj, S.P., den Braver, M.W., Baze, A., Decorde, J., Fonsi, M., Bachellier, P., Vermeulen, N.P.E., Commandeur, J.N.M., Richert, L., Vos, J.C., 2017. Direct comparison of UDP-glucuronosyltransferase and cytochrome P450 activities in human liver microsomes, plated and suspended primary human hepatocytes from five liver donors. Eur. J. Pharm. Sci. 109, 96–110. https://doi.org/10.1016/j.ejps.2017.07.032.

Dong, J.Q., Smith, P.C., 2009. Glucuronidation and covalent protein binding of benoxaprofen and flunoxaprofen in sandwich-cultured rat and human hepatocytes. Drug Metab. Dispos. 37, 2314–2322. https://doi.org/10.1124/dmd.109.028944.

ECHA, 2008. Member State Committee Support Document for Identification of Hexabromocyclododecane and All Major Diastereoisomers Identified As a Substance of Very High Concern.

Ema, M., Fujii, S., Hirata-Koizumi, M., Matsumoto, M., 2008. Two-generation reproductive toxicity study of the flame retardant hexabromocyclododecane in rats. Reprod. Toxicol. 25, 335–351. https://doi.org/10.1016/j.reprotox.2007.12.004.

Erratico, C., Zheng, X., Van Den Eede, N., Tomy, G., Covaci, A., 2016. Stereoselective metabolism of α-, β-, and γ-hexabromocyclododecanes (HBCDs) by human liver microsomes and CYP3A4. Environ. Sci. Technol. 50, 8263–8273. https://doi.org/10.1021/acs.est.6b01059.

Farmahin, R., Marie, A., Gagné, R., Rowan-carroll, A., Kuo, B., Williams, A., Curran, I., Yauk, C.L., 2019. Hepatic transcriptional dose-response analysis of male and female Fischer rats exposed to hexabromocyclododecane. Food Chem. Toxicol. 133, 110262 https://doi.org/10.1016/j.fct.2018.12.032.

Feder, M.E., Walser, J.C., 2005. The biological limitations of transcriptomics in elucidating stress and stress responses. J. Evol. Biol. 18, 901–910. https://doi.org/10.1111/j.1420-9101.2005.00921.x.

Fery, Y., Buschauer, I., Salzig, C., Lang, P., Schrenk, D., 2009. Technical pentabromodiphenyl ether and hexabromocyclododecane as activators of the pregnane-X-receptor (PXR). Toxicology 264, 45–51. https://doi.org/10.1016/j.tox.2009.07.009.

Foster, J.R., Tinwell, H., Melching-Kollmuss, S., 2021. A review of species differences in the control of, and response to, chemical-induced thyroid hormone perturbations leading to thyroid cancer. Arch. Toxicol. 95, 807–836. https://doi.org/10.1007/s00204-020-02961-6.

Gannon, A.M., Moreau, M., Farmahin, R., Thomas, R.S., Barton-Maclaren, T.S., Nong, A., Curran, I., Yauk, C.L., 2019. Hexabromocyclododecane (HBCD): a case study applying tiered testing for human health risk assessment. Food Chem. Toxicol. 131, 110581 https://doi.org/10.1016/j.fct.2019.110581.

Gerets, H.H.J., Tilmant, K., Gerin, B., Chanteux, H., Depelchin, B.O., Dhalluin, S., Atienzar, F. a, 2012. Characterization of primary human hepatocytes, HepG2 cells, and HepaRG cells at the mRNA level and CYP activity in response to inducers and their predictivity for the detection of human hepatotoxins. Cell Biol. Toxicol. 28, 69–87. https://doi.org/10.1007/s10565-011-9208-4.

Germer, S., Piersma, A.H., Van Der Ven, L., Kamyschnikow, A., Fery, Y., Schmitz, H.J., Schrenk, D., 2006. Subacute effects of the brominated flame retardants hexabromocyclododecane and tetrabromobisphenol A on hepatic cytochrome P450 levels in rats. Toxicology 218, 229–236. https://doi.org/10.1016/j.tox.2005.10.019.

Gross-Steinmeyer, K., Stapleton, P.L., Tracy, J.H., Bammler, T.K., Lehman, T., Strom, S.C., Eaton, D.L., 2005. Influence of Matrigel-overlay on constitutive and inducible expression of nine genes encoding drug-metabolizing enzymes in primary human hepatocytes. Xenobiotica 35, 419–438. https://doi.org/10.1080/00498250500137427.

Guillouzo, A., Corlu, A., Aninat, C., Glaise, D., Morel, F., Guguen-Guillouzo, C., 2007. The human hepatoma HepaRG cells: a highly differentiated model for studies of liver metabolism and toxicity of xenobiotics. Chem. Biol. Interfaces 168, 66–73. https://doi.org/10.1016/j.cbi.2006.12.003.

Gülden, M., Mörchel, S., Seibert, H., 2001. Factors influencing nominal effective concentrations of chemical compounds in vitro: cell concentration. Toxicol. Vitr. 15, 233–243.

Gunness, P., Mueller, D., Shevchenko, V., Heinzle, E., Ingelman-Sundberg, M., Noor, F., 2013a. 3D organotypic cultures of human HepaRG cells: a tool for in vitro toxicity studies. Toxicol. Sci. 133, 67–78. https://doi.org/10.1093/toxsci/kft021.

Gunness, P., Mueller, D., Shevchenko, V., Heinzle, E., Ingelman-Sundberg, M., Noor, F., 2013b. 3D organotypic cultures of human HepaRG cells: a tool for in vitro toxicity studies. Toxicol. Sci. 133, 67–78. https://doi.org/10.1093/toxsci/kft021.

Hamers, T., Kamstra, J.H., Sonneveld, E., Murk, A.J., Kester, M.H.A., Andersson, P.L., Legler, J., Brouwer, A., 2006. In vitro profiling of the endocrine-disrupting potency of brominated flame retardants. Toxicol. Sci. 92, 157–173. https://doi.org/10.1093/toxsci/kfj187.

Hennemann, G., Docter, R., Friesema, E.C.H., De Jong, M., Krenning, E.P., Visser, T.J., 2001. Plasma membrane transport of thyroid hormones and its role in thyroid hormone metabolism and bioavailability. Endocr. Rev. 22, 451–476. https://doi.org/10.1210/edrv.22.4.0435.

Hyland, R., Osborne, T., Payne, A., Kempshall, S., Logan, Y.R., Ezzeddine, K., Jones, B., 2009. In vitro and in vivo glucuronidation of midazolam in humans. Br. J. Clin. Pharmacol. 67, 445–454. https://doi.org/10.1111/j.1365-2125.2009.03386.x.

Jansen, J., Friesema, E.C.H., Milici, C., Visser, T.J., 2005. Thyroid hormone transporters in health and disease. Thyroid 15. https://doi.org/10.1089/thy.2005.15.757.

Koop, D.R., Casazza, J.P., 1985. Identification of ethanol-inducible P-450 isozyme 3a as the acetone and acetol monooxygenase of rabbit microsomes. J. Biol. Chem. 260, 13607–13612. https://doi.org/10.1016/s0021-9258(17)38768-9.

Kramer, N.I., Di Consiglio, E., Blaauboer, B.J., Testai, E., 2015. Biokinetics in repeated-dosing in vitro drug toxicity studies. Toxicol. Vitr. 30, 217–224. https://doi.org/10.1016/j.tiv.2015.09.005.

Kühnlenz, J., Karwelat, D., Steger-Hartmann, T., Raschke, M., Bauer, S., Vural, O., Marx, U., Tinwell, H., Bars, R., 2022. A microfluidic thyroid-liver platform to assess chemical safety in humans. ALTEX. https://doi.org/10.14573/altex.2108261.

Lauschke, V.M., Hendriks, D.F.G., Bell, C.C., Andersson, T.B., Ingelman-Sundberg, M., 2016. Novel 3D culture systems for studies of human liver function and assessments of the hepatotoxicity of drugs and drug candidates. Chem. Res. Toxicol. 29, 1936–1955. https://doi.org/10.1021/acs.chemrestox.6b00150.

Legendre, C., Hori, T., Loyer, P., Aninat, C., Ishida, S., Glaise, D., Lucas-clerc, C., Boudjema, K., Guguen-guillouzo, C., Corlu, A., Morel, F., 2009. Drug-metabolising enzymes are down-regulated by hypoxia in differentiated human hepatoma HepaRG cells: HIF-1 a involvement in CYP3A4 repression. Eur. J. Cancer 45, 2882–2892. https://doi.org/10.1016/j.ejca.2009.07.010.

Li, L., Wania, F., 2018. Elucidating the variability in the hexabromocyclododecane diastereomer profile in the global environment. Environ. Sci. Technol. 52, 10532–10542. https://doi.org/10.1021/acs.est.8b03443.

Limonciel, A., Ates, G., Carta, G., Wilmes, A., Watzele, M., Shepard, P.J., VanSteenhouse, H.C., Seligmann, B., Yeakley, J.M., van de Water, B., Vinken, M., Jennings, P., 2018. Comparison of base-line and chemical-induced transcriptomic responses in HepaRG and RPTEC/TERT1 cells using TempO-Seq. Arch. Toxicol. 92, 2517–2531. https://doi.org/10.1007/s00204-018-2256-2.

Liu, C., Wang, C., Yan, M., Quan, C., Zhou, J., Yang, K., 2012. PCB153 disrupts thyroid hormone homeostasis by affecting its biosynthesis, biotransformation, feedback regulation, and metabolism. Horm. Metab. Res. 44, 662–669. https://doi.org/10.1055/s-0032-1311569.

Love, M.I., Huber, W., Anders, S., 2014. Moderated estimation of fold change and dispersion for RNA-seq data with DESeq2. Genome Biol. 15, 550. https://doi.org/10.1186/s13059-014-0550-8.

Morose, G., 2006. An overview of alternatives to tetrabromobisphenol A (TBBPA) and hexabromocyclododecane (HBCD). A Plublication of the Lowell Center for Sustainable Production, A Publication of the Lowell Center for Sustainable Production.

Mueller, D., Krämer, L., Hoffmann, E., Klein, S., Noor, F., 2014. 3D organotypic HepaRG cultures as in vitro model for acute and repeated dose toxicity studies. Toxicol. Vitr. 28, 104–112. https://doi.org/10.1016/j.tiv.2013.06.024.

Nguyen, H.Q., Kimoto, E., Callegari, E., Obach, R.S., 2016. Mechanistic modeling to predict midazolam metabolite exposure from in vitro data. Drug Metab. Dispos. 44, 781–791. https://doi.org/10.1124/dmd.115.068601.

Nixon, M. and, 1997. Hexabromocyclododecane (HBCD): Determination of noctanol/water partition coefficient.

Noyes, P.D., Friedman, K.P., Browne, P., Haselman, J.T., Gilbert, M.E., Hornung, M.W., Barone, S., Crofton, K.M., Laws, S.C., Stoker, T.E., Simmons, S.O., Tietge, J.E., Degitz, S.J., 2019. Evaluating chemicals for thyroid disruption: Opportunities and challenges with in Vitro testing and adverse outcome pathway approaches. Environ. Health Perspect. 127. https://doi.org/10.1289/EHP5297.

Ohnaus, E.E., Burgi, H., Burger, A., Studer, H., 1981. The effect of antipyrine, phenobarbitol and rifampicin on thyroid hormone metabolism in man. Eur. J. Clin. Investig. 11, 381–387. https://doi.org/10.1111/j.1365-2362.1981.tb02000.x.

Pavek, P., 2016. Pregnane X receptor (PXR)-mediated gene repression and cross-talk of PXR with other nuclear receptors via coactivator interactions. Front Pharmacol. 7, 1–16. https://doi.org/10.3389/fphar.2016.00456.

Plummer, S., Beaumont, B., Elcombe, M., Wallace, S., Wright, J., Mcinnes, E.F., Currie, R. A., Cowie, D., 2021. Species differences in phenobarbital-mediated UGT gene induction in rat and human liver microtissues. Toxicol. Rep. 8, 155–161. https://doi.org/10.1016/j.toxrep.2020.12.019.

Pomponio, G., Savary, C.C., Parmentier, C., Bois, F., Guillouzo, A., Romanelli, L., Richert, L., di Consiglio, E., Testai, E., 2015. In vitro kinetics of amiodarone and its major metabolite in two human liver cell models after acute and repeated treatments. Toxicol. Vitr. 30, 36–51. https://doi.org/10.1016/j.tiv.2014.12.012.

Proença, S., Escher, B.I., Fischer, F.C., Fisher, C., Grégoire, S., Hewitt, N.J., Nicol, B., Paini, A., Kramer, N.I., 2021. Effective exposure of chemicals in in vitro cell systems: a review of chemical distribution models. Toxicol. Vitr. 73. https://doi.org/10.1016/j.tiv.2021.105133.

Ramaiahgari, S.C., Waidyanatha, S., Dixon, D., DeVito, M.J., Paules, R.S., Ferguson, S.S., 2017. Three-dimensional (3D) HepaRG spheroid model with physiologically-relevant xenobiotic metabolism competence and hepatocyte functionality for liver toxicity screening. Toxicol. Sci. 1, 1–35. https://doi.org/10.1093/toxsci/kfx122.

Richardson, V.M., Ferguson, S.S., Sey, Y.M., Devito, M.J., 2014. In vitro metabolism of thyroxine by rat and human hepatocytes. Xenobiotica 44, 391–403. https://doi.org/10.3109/00498254.2013.847990.

Schomburg, L., 2012. Selenium, selenoproteins and the thyroid gland: Interactions in health and disease. Nat. Rev. Endocrinol. 8, 160–171. https://doi.org/10.1038/nrendo.2011.174.

Shizu, R., Ezaki, K., Sato, T., Sugawara, A., Hosaka, T., Sasaki, T., Yoshinari, K., 2021. Pxr suppresses pparα-dependent hmgcs2 gene transcription by inhibiting the interaction between pparα and pgc1α. Cells 10. https://doi.org/10.3390/cells10123550.

Shockley, K.R., Cora, M.C., Malarkey, D.E., Jackson-Humbles, D., Vallant, M., Collins, B. J., Mutlu, E., Robinson, V.G., Waidyanatha, S., Zmarowski, A., Machesky, N., Richey, J., Harbo, S., Cheng, E., Patton, K., Sparrow, B., Dunnick, J.K., 2020. Comparative toxicity and liver transcriptomics of legacy and emerging brominated flame retardants following 5-day exposure in the rat. Toxicol. Lett. 332, 222–234. https://doi.org/10.1016/j.toxlet.2020.07.016.

Soars, M.G., Petullo, D.M., Eckstein, J.A., Kasper, S.C., Wrighton, S.A., 2004. An assessment of UDP-glucuronosyltransferase induction using primary human hepatocytes. Drug Metab. Dispos. 32, 140–148. https://doi.org/10.1124/dmd.32.1.140.

Tong, Z., Li, H., Goljer, I., McConnell, O., Chandrasekaran, A., 2007. In vitro glucuronidation of thyroxine and triiodothyronine by liver microsomes and recombinant human UDP-glucuronosyltransferases. Drug Metab. Dispos. 35, 2203–2210. https://doi.org/10.1124/dmd.107.016972.

van der Spek, A.H., Fliers, E., Boelen, A., 2017. The classic pathways of thyroid hormone metabolism. Mol. Cell Endocrinol. 458, 29–38. https://doi.org/10.1016/j.mce.2017.01.025.

van der Ven, L.T.M., Verhoef, A., van de Kuil, T., Slob, W., Leonards, P.E.G., Visser, T.J., Hamers, T., Herlin, M., Håkansson, H., Olausson, H., Piersma, A.H., Vos, J.G., 2006. A 28-day oral dose toxicity study enhanced to detect endocrine effects of hexabromocyclododecane in Wistar rats. Toxicol. Sci. 94, 281–292. https://doi.org/10.1093/toxsci/kfl113.

Varga, T., Czimmerer, Z., Nagy, L., 2011. PPARs are a unique set of fatty acid regulated transcription factors controlling both lipid metabolism and inflammation. Biochim Biophys. Acta Mol. Basis Dis. 1812, 1007–1022. https://doi.org/10.1016/j.bbadis.2011.02.014.

Vorrink, S.U., Domann, F.E., 2014. Regulatory crosstalk and interference between the and hypoxia sensing pathways at the AhR-ARNT-HIF1α signaling node. Chem. Biol. Interact. 218, 82–88. https://doi.org/10.1016/j.cbi.2014.05.001.

Wang, F., Zhang, H., Geng, N., Zhang, B., Ren, X., Chen, J., 2016. New insights into the cytotoxic mechanism of hexabromocyclododecane from a metabolomic approach. Environ. Sci. Technol. 50, 3145–3153. https://doi.org/10.1021/acs.est.5b03678.

Wang, J., Vasaikar, S., Shi, Z., Greer, M., Zhang, B., 2017. WebGestalt 2017: a more comprehensive, powerful, flexible and interactive gene set enrichment analysis toolkit. Nucleic Acids Res. 45, W130–W137. https://doi.org/10.1093/nar/gkx356.

Wang, X.S., Tan, X., Zhang, Y., Hu, X. xin, Shen, C., Huang, Y. ying, Fu, H. ling, Yu, R. han, He, C. tao, 2021. The enantiomer-selective metabolism of hexabromocyclododecanes (HBCDs) by human HepG2 cells. Sci. Total Environ. 768, 144430 https://doi.org/10.1016/j.scitotenv.2020.144430.

Wang, Z., Luo, X., Anene-Nzelu, C., Yu, Y., Hong, X., Singh, N.H., Xia, L., Liu, S., Yu, H., 2014. HepaRG culture in tethered spheroids as an in vitro three-dimensional model for drug safety screening. J. Appl. Toxicol. https://doi.org/10.1002/jat.3090.

Wei, Y., Tang, C., Sant, V., Li, S., Poloyac, S.M., Xie, W., 2016. A molecular aspect in the regulation of drug metabolism: does PXR-induced enzyme expression always lead to functional changes in drug metabolism? Curr. Pharmacol. Rep. 2, 187–192. https://doi.org/10.1007/s40495-016-0062-1.

Westerink, W.M., Schoonen, W.G.E.J., 2007. Phase II enzyme levels in HepG2 cells and cryopreserved primary human hepatocytes and their induction in HepG2 cells. Toxicol. Vitr. 21, 1592–1602. https://doi.org/10.1016/j.tiv.2007.06.017.

Zhang, J., Williams, T.D., Abdallah, M.A.E., Harrad, S., Chipman, J.K., Viant, M.R., 2015. Transcriptomic and metabolomic approaches to investigate the molecular responses of human cell lines exposed to the flame retardant hexabromocyclododecane (HBCD). Toxicol. Vitr. 29, 2116–2123. https://doi.org/10.1016/j.tiv.2015.08.017.

Zhang, Y.X., Shen, C.H., Lai, Q.L., Fang, G.L., Ming, W.J., Lu, R.Y., Ding, M.P., 2016. Effects of antiepileptic drug on thyroid hormones in patients with epilepsy: a meta-analysis. Seizure 35, 72–79. https://doi.org/10.1016/j.seizure.2016.01.010.

Zhu, A., Ibrahim, J.G., Love, M.I., 2019. Heavy-Tailed prior distributions for sequence count data: Removing the noise and preserving large differences. Bioinformatics 35, 2084–2092. https://doi.org/10.1093/bioinformatics/bty895.